Lamb waves recorded in microseismic monitoring wellbores

Andy St-Onge, Department of Geoscience, University of Calgary

G e o C o n v e n t i o n   2 0 1 2 : V i s i o n

Abstract

Microseismic data recorded during the hydraulic fracturing of two horizontal wells has been examined to identify coherent signal and noise. The objective was to better understand events recorded on the data. The signal and noise events were identified by their occurrence rate, apparent velocity and frequency content. Lamb waves have been identified on both datasets. They have high amplitude relative to the signal and apparent velocities similar to P waves.

Introduction

Microseismic data is being recorded to try to locate fractures induced by the hydraulic fracturing of horizontal wells. Three component geophones placed down cased offsetting vertical wellbores can be used to record the data. Microseismic data are usually continuously recorded at high sample rates compared to surface seismic acquisition.

A cemented wellbore with steel casing has the potential to propagate many type of waves. P and S waves can be transmitted in a wellbore within the steel casing, or the cement (Raggio, et. al., 2007). The P wave can also be transmitted within the fluid within the wellbore. There are many types of surface waves that can be recorded in a wellbore.   Bokov and Ionov (2001) discuss the modelling of a microseismic event to create a tube wave propagating in a borehole. Stevens and Day (1986) discuss Stoneley waves as a tool to measure shear velocities. Lamb waves are a type of surface wave that can propagate in a wellbore. The recording of Lamb waves on microseismic data is the focus of this paper.

All of the waves in a borehole have characteristic (but maybe not unique) apparent velocities and dominant frequencies. For example, P waves can travel in strong steel at V_P = 5,700 to 6,100 m/sec, and S waves can travel from V_S = 3,220 to 3,280 m/sec (Raggio et. al., 2007). Rama Rao and Vandiver (1999) measure three modes of tube waves with velocities ranging from 750 to 1,530 m/sec and frequencies up to 1000 Hz. Lamb waves have a velocity that is determined by the cross section profile of the borehole; this calculation is discussed below. It may be possible to identify all wave types by their recorded apparent velocity, dominant frequency and dispersion characteristics.

Lamb waves have been used for a number of years in the non-destructive evaluation (NDE) of pipelines. The high frequency (in the MHz. range) waves are intentionally generated and their attenuation is measured as they travel along underground pipelines. The attenuation is interpreted and compared to characteristic results to look for problems such as cracks or borehole irregularities. There has been little mention in recent microseismic publications on Lamb waves recorded on microseismic data. The data presented here are thought to be low frequency Lamb waves generated and recorded during the monitoring of hydraulic fracturing.

The microseismic data

The Microseismic Industry Consortium (MIC) is a joint effort between the University of Calgary, the University of Alberta and 21 sponsors. The MIC has access to eight microseismic datasets recorded throughout western Canada. The data were sampled at rates as low as 0.25 msec, which is equivalent to a Nyquist frequency of 2000 Hz. Signal data observed by MIC contains frequencies approaching 800 Hz. All of the data were recorded in boreholes lined with steel and cement to the strata. The boreholes range in depth from 1200 to 3100m. Finally, the MIC has been working with data recorded with geophone spacing ranging from 11 to 15 meters in strings of seven to 12 geophones.

Lamb waves

Lamb waves are a type of elastic guided wave that travels along a plate surface or along a cylindrical surface. They were first described by Lamb (1917). In a cylinder such as a cased wellbore, the coupled longitudinal and transverse particle motion result in three possible modes of travel. These modes are longitudinal, torsional and flexural, as shown in Figure 1. Lamb waves are dispersive, meaning that different frequencies propagate at different speeds. Dispersion curves are used to describe the apparent velocity of Lamb waves. One dispersion curve is shown in Figure 2 (from Giurgiutiu et. al., 2003).
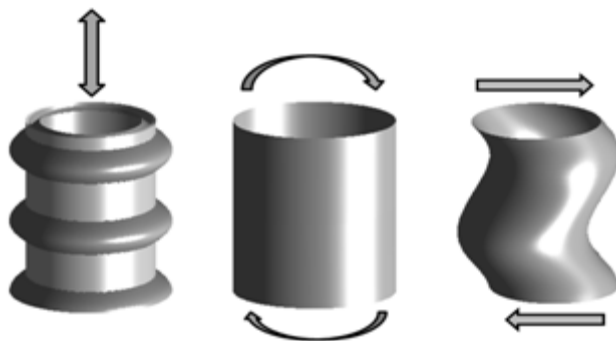

Figure 1- Particle motion for Lamb waves in a cylinder include longitudinal, torsional and flexural modes.
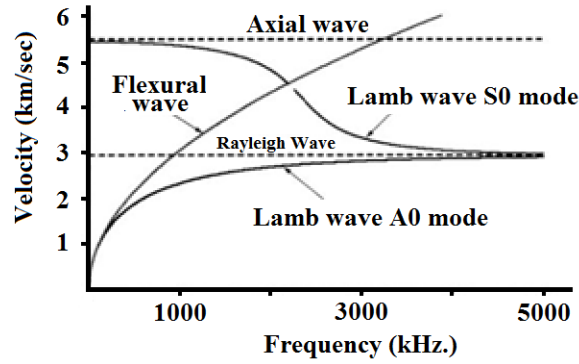
Figure 2- An example of dispersion curves for Lamb waves in a 1 mm thick aluminum plate (from Giurgiutiu and Lyshevski (2003)).

Lamb waves can occur in an infinite number of modes at higher frequencies. Formulation of the dispersion curves comes from the solution of the period equation, as presented in Achenbach (1999), for symmetric and asymmetric waves, respectively:

$$\frac{\tan(qh)}{\tan(ph)} = -\frac{4k^2 pq}{\left(q^2 - k^2\right)^2} \quad \text{(Symmetric)} \tag{1}$$

$$\frac{\tan(qh)}{\tan(ph)} = -\frac{\left(q^2 - k^2\right)^2}{4k^2 pq} \quad \text{(Asymmetric)} \tag{2}$$

$$p^2 = \frac{\omega^2}{c_L^2} - k^2, \quad q^2 = \frac{\omega^2}{c_T^2} - k^2$$

$$c_L = \sqrt{\frac{\lambda + 2\mu}{\rho}}, \quad c_T = \sqrt{\frac{\mu}{\rho}}$$

$$\mu = \frac{E}{2(1+v)}, \quad \lambda = \frac{Ev}{(1-2v)(1+v)}$$

Where: E = Young's modulus v = Poisson's ratio   ω = circular frequency
        k = wave number
        V_P = compression velocity V_S = shear velocity   and   μ, λ = Lame constants

The solution for Equations 1 and 2 can be evaluated numerically. At seismic frequencies (below 800 Hz., usually only two modes exist, the first torsional and longitudinal modes. The velocities for these modes can be calculated numerically, as discussed below.

Results - microseismic survey # 1

Microseismic survey # 1 recorded six hours of data at a 0.00025 msec sample rate. Twenty four traces of three component seismic data were recorded, in a borehole with cross sectional parameters shown in Table 1 and Figure 3. Over 60 events similar to the Lamb wave in Figure 5 were observed on potential events that were identified on the six hour time series. These potential events were extracted using an amplitude threshold algorithm; there may be more Lamb wave events recorded but not detected by this algorithm.

The values from Table 1 were used to calculate a dispersion curve for the wellbore. The software is provided online at the Geophysics Software Library and is from Karpfinger (2009). Figure 4 shows the results of the program. Burago et. al. (1980) analytically calculated the velocity of the L(0,1) mode at zero frequency for a cross sectional area as shown in Figure 3. Both solutions are a function of V_p and density for the borehole fluid and the casing, the radii of the casing, V_s for the steel casing and the shear modulus of the casing and the casing cement. Burago et. al. (1980) make the point that the medium outside of the casing only affects the low frequency solution through the shear modulus of the cement.

annular area	α_i	β_i	ρ_i	Radii, r_i	
				Survey 1	Survey 2
Inner Fluid	1,500 m/sec	-	1.00 gm/cm^3	0.100 m	0.100 m
Steel Casing	5,930	3,200 m/sec	7.85	0.120	0.120
Borehole Cement	4,200	2,400	2.20	0.250	0.250
Rock Formation	4,800	2,800	2.60	2.700	2.700

Table 1 – the P and S wave velocities (α, β) and densities (ρ) used for both surveys. Refer to Figure 3.
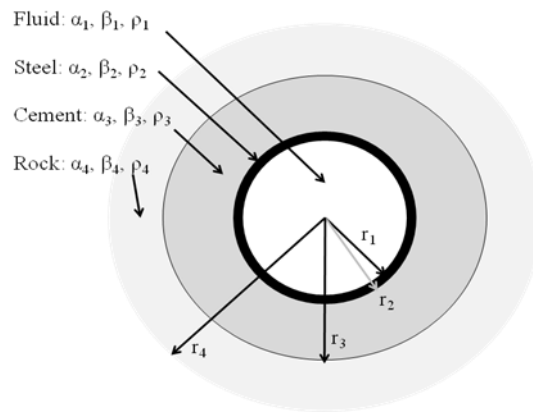
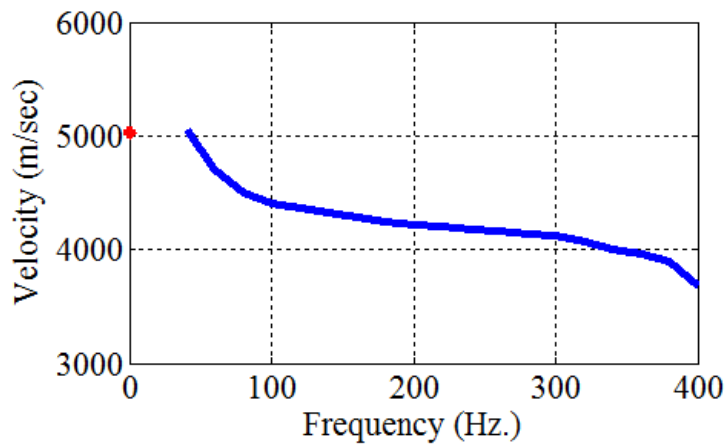Figure 3- Cross section through a wellbore.

Figure 4- Dispersion curve calculated for the geometries for both examples presented here. At a frequency of about 40 Hz, the velocity of the L(0,1) longitudinal mode is predicted to be about 5,200 m/sec. The blue curve is estimated using software from Karpfinger (2009); the red dot is a D.C. estimate from Burago, et. Al. (1980).

Consider Figure 5. There is a initially a high amplitude upgoing wave on both horizontal channels, followed by upgoing energy on the vertical channels. The dominant frequency on the vertical channels is about 40 Hz. The low frequency of the event is apparent on Figure 4. At the top of the assembly, the upgoing P wave reflects and starts going down the wellbore.
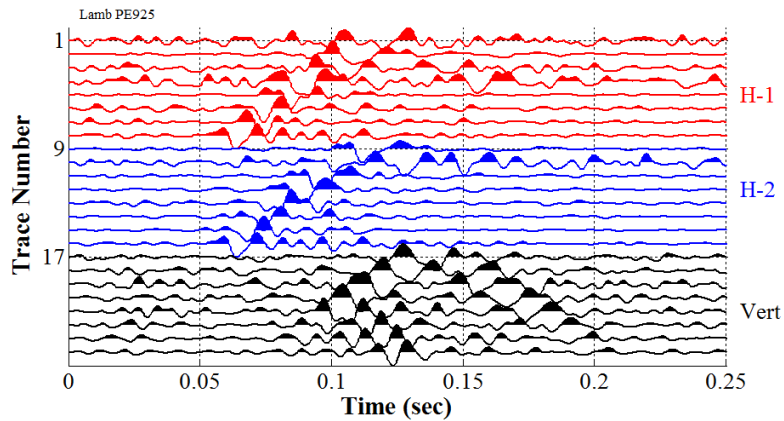
Figure 5- A Lamb wave event from the NEBC microseismic dataset. The data are plotted after a 5/10-100/140 Hz. Bandpass filter. The data has been phase rotated on the H-2 and H-2 components. The lower traces are deeper in the wellbore.

Figure 6 is Figure 5 replotted without trace equalization. Initially, high amplitude energy is recorded by the horizontal geophones. This energy travels up the wellbore at a velocity of about 5,200 m/sec. Between the fourth and fifth geophone position, and at the uppermost geophone location, downgoing P wave energy is initiated. The downgoing P wave at 0.14 sec. on trace 16 at the bottom of the wellbore is very high amplitude and travels at about 3,800 m/sec. The 5,200 m/sec is thought to be a longitudinal L(0,1) mode Lamb wave.   The 3,800 m/sec event could be the T(0,1) torsional mode Lamb wave.
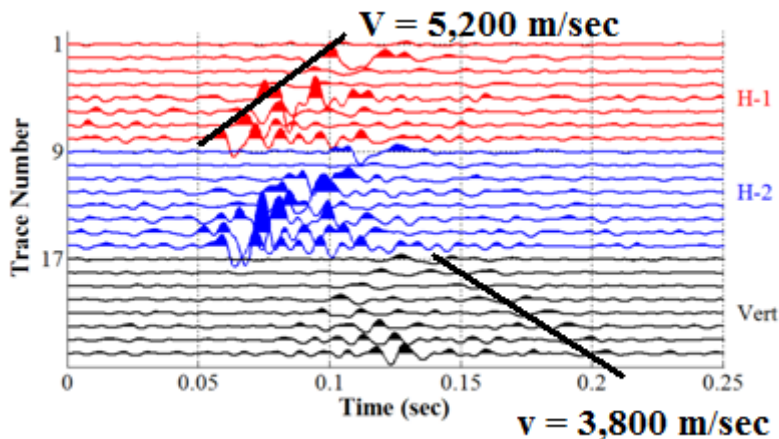

Figure 6- A replot of Figure 5 without trace equalization.

Microseismic survey # 2

Microseismic survey # 2 recorded six hours of 36 traces of three component data at a 0.0005 msec sample rate. Numerous events similar to the Lamb wave in Figure 7 were observed on the three hour time series. The energy on the vertical traces is highly dispersive. This was confirmed with frequency amplitude spectra (not shown here) showing that the peak frequency decreased to 50 Hz. (from 80 Hz.) over a 210 m distance. Figure 8 shows the group velocity versus frequency plot for the vertical traces in Figure 7.
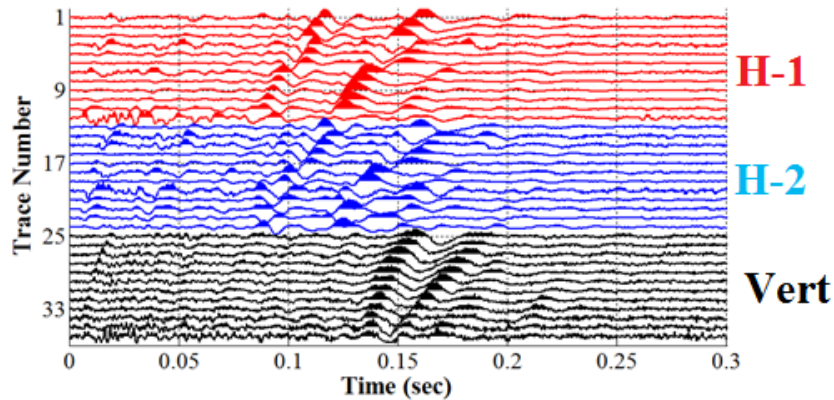
.

Figure 7- A Lamb wave event from microseismic dataset #2. The data are plotted after a 5/10-200/260 Hz. Bandpass filter. The lower traces are deeper in the wellbore.
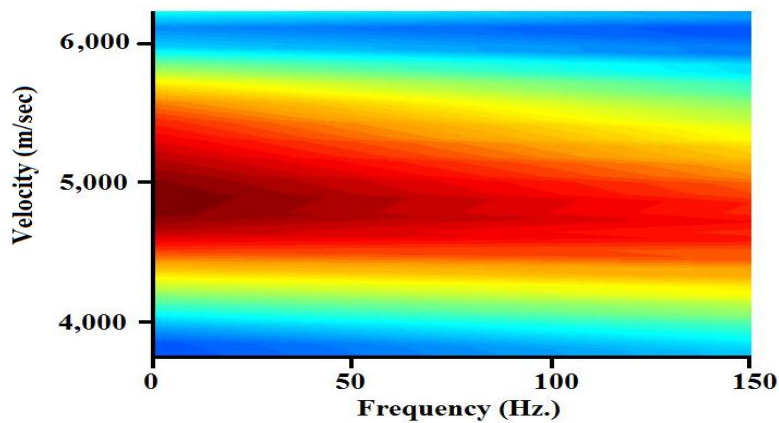

Figure 8- A group velocity versus frequency (dispersion curve) for the vertical traces shown in Figure 7. The velocity dependence on frequency is typical for a Lamb wave. The plot indicates an average velocity of about 5,000 m/sec.

Discussion

The Lamb waves observed in the datasets and presented here always starts near the bottom of the wellbore.   Perhaps an incident P or S wave initiates the Lamb wave at or near the bottom of the borehole. After this, the waves travel upward. It is apparent in Figures 5 and 6 that some of the Lamb waves can be reflected to downward travelling waves.   Something initiates a downgoing wave at the fourth or fifth geophone position. This could be a geological impedance contrast; however, there does not appear to be a large impedance contrast at this depth. The wellbore casing may have a metal centralizer at this location. Finally, a poorly cemented casing may initiate the reflection (Leary, et. al., 1990).

The Lamb waves have characteristic properties of transmission within the wellbore and have been observed over 60 times in one hydraulic fracture monitoring.   They are dispersive and travel at velocities of about 5,000 m/sec (for the L(0,1) mode). Figure 7 shows one cause for concern. The combination of the Lamb wave velocity and dispersion with distance combine to make the arrival 'appear' to have normal moveout. This may cause an automatic picking program to detect and try to geolocate such events.

Conclusions

Microseismic data recorded during the hydraulic fracturing of two horizontal wells has been examined to identify coherent signal and noise. The objective was to better understand events recorded on the data. The signal and noise were identified by their rate of occurrence, apparent velocity and frequency content. Lamb waves were identified on both datasets. They have high amplitude relative to the signal and apparent velocities similar to P and S wave arrivals.

Acknowledgments

References

Achenbach, J. D., 1973, Wave propagation in elastic solids, North Holland, Amsterdam.

Alleyne, D.N. and Cawley, P. 'The excitation of Lamb waves in pipes using dry coupled piezoelectric transducers', J NDE, Vol 15, pp11-20, 1996.

Aristegui, C., Lowe, M. J. S., and Cawley, P., 2001, Guided waves in a fluid filled pipe surrounded by different fluids, Ultrasonics, 39 (2001) 367-375

Burago, N. A., Ibatov, A. S., Krauklis, P. V., and Krauklis, L. A., 1980, Dispersion of tube and Lamb waves recorded in acoustic logging, Journal of Mathematical Sciences, Volume 20, No. 5, pp. 2401-2407.

Chen, X., and Wan, M., 2005, Parameter measurement of the cylindrically curved thin layer using low-frequency circumferential Lamb waves, Ultrasonics, Volume 43 (2005), 357-364

Clorennec, D., Prada, C., and Royer, D., 2007, Local and noncontact measurements of bulk acoustic wave velocities in thin isotropic plates and shells using zero group velocity Lamb modes, Journal of Applied Physics, 101, (3)

Galvagni, A., and Cawley, P., The reflection of guided waves from simple supports on pipes, J. Acoust. Soc. Am., **129** (4), pp. 1869-1880.

Gibson, A., and Popovics, J., 2005, Lamb wave basis for impact-echo method analysis, Journal of Engineering Mechanics, Vol. 131, No. 4, pp. 438-443

Giurgiutiu, V. and Lyshevski, S., 2003, Micromechatronics: Modeling, Analysis and Design with MATLAB, CRC Press, New York

Karpfinger, F., 2009, Modelling borehole wave signatures in elastic and poroelastic media with spectral method, Ph. D. Thesis, Curtin University of Technology, Australia

Long, R., Lowe, M., and Cawley, P., 2003, Attenuation characteristics of the fundamental modes that propagate in buried iron water pipes, Ultrasonics, 41 (2003) 509-519

Raggio, L., Etcheverry, J., and Bonadeo, N., 2007, Determination of acoustic shear and compressional wave velocities for steel samples by impulse excitation of vibrations, IV Conferencia Panimericana de END, Buenos Aires, October 2007

Rama Rao, V. N., and Vandiver, J., K., 1999, Acoustics of fluid-filled boreholes with pipe: Guided propagation and radiation, J. Acoust. Soc. Am., Vol. 105, No. 6, pp. 3057-3066

Shin, Y., Chung, J., Kladias, N., Panides, E., Domoto, G., and Grigoropoulos P., 2005, Compressible flow of liquid in a standing wave tube, J. Fluid Mech. (2005), vol. 536, pp. 321-345.

Stevens, J. L. and Day, S., M., 1986, Shear velocity logging in slow formations using the Stoneley wave, Geophysics **51**, 137–147.

Tadeu, A., and Santos, P., 2001, 3-D wave propagation in fluid filled irregular boreholes in elastic formations, Soil Dynamics and Earthquake Engineering, 21 (2001), pp. 499-517.

Thien, A. B. 2006, Pipeline structural health monitoring using macro-fibre composite active sensors, M. Sc. Thesis, University of Cincinnati